

Ignition of Hydrogen-Air Mixtures Under Volumetric Expansion

R. Mével^{1,2}, J. Melguizo-Gavilanes³ and D. Davidenko⁴

¹**Center for Combustion Energy, Tsinghua University, Beijing, China**

²**Department of Automotive Engineering, Tsinghua University, Beijing, China**

³**California Institute of Technology, Pasadena, CA, USA**

⁴**The French Aerospace Lab ONERA, Palaiseau, France**

mevel@mail.tsinghua.edu.cn

ABSTRACT

A better understanding of chemical kinetics under volumetric expansion is important for a number of situations relevant to industrial safety including detonation diffraction and direct initiation, reflected shock-ignition at obstacles, ignition behind a decaying shock, etc. In the present study, the ignition of stoichiometric hydrogen-air mixtures has been studied using 0-D numerical simulations with time-dependent specific volume. The competition between chemical energy release and expansion-induced cooling has been characterized for different cooling rates and mathematical forms describing the shock decay rate. The critical conditions for reaction quenching were systematically determined, and the thermo-chemistry dynamics has been analyzed near the critical conditions.

1. INTRODUCTION

Improved understanding of ignition mechanisms behind decaying shock waves is important not only from a scientific perspective but is also relevant in many practical applications. This generic/canonical problem plays an important role in situations such as direct initiation of detonations by blast waves [1], detonation propagation through abrupt area changes [2], also commonly referred to as detonation diffraction, and shock-induced diffusion ignition [3]. All of the previously mentioned examples could readily arise in industrial settings after accidental releases of hydrogen from high pressure fuel tanks or containers. While the idea that chemical reactions can altogether be quenched behind decaying shock waves was first suggested decades ago [4], and many theoretical and numerical attempts have been made to further understand the gas dynamical mechanisms driving this behavior (namely investigating the role of gas dynamical expansions [5], curvature [6] and shock unsteadiness [1]), the majority of the work performed has been restricted to a global understanding of the coupling of chemical heat release with the flow through simplified descriptions of the chemistry. Only a few researchers [3, 1] have used detailed chemistry but their analyses have been limited to examining temporal and spatial distributions of species mass fractions during ignition. The goal of the present study is to extend the previous work by performing a systematic characterization of the impact of volumetric expansion on the ignition process and on the chemical pathways of premixed stoichiometric hydrogen-air mixtures for a wide range of conditions. The manuscript is structured as follows: a detailed description of the methodology and calculation procedure is presented in section 2; section 3 covers the results and discussion; and closing remarks are presented in section 4.

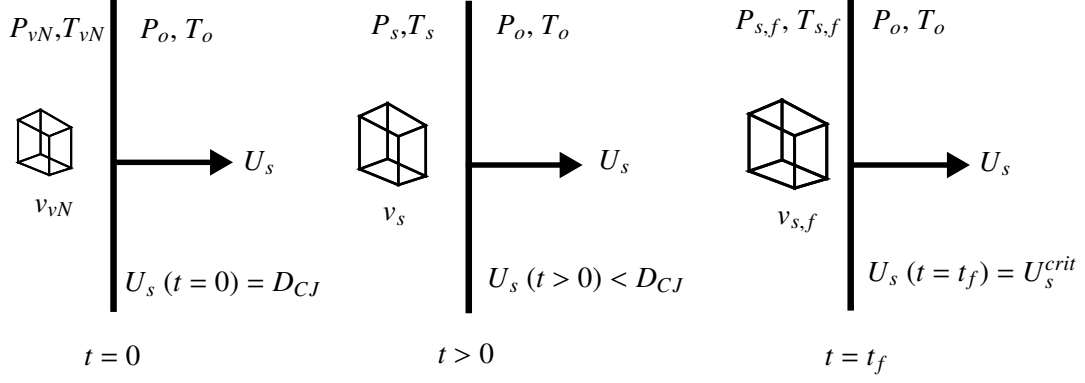


Figure 1: Schematic of problem definition showing initial conditions ahead of shock, and post-shock conditions with parcel of gas expanding as the shock velocity decays.

2. METHODOLOGY AND CALCULATION PROCEDURE

2.1. Problem definition

The modeled problem is related to the reaction zone behind a decaying shock wave propagating in a combustible mixture. The problem considered here corresponds to a shock initially propagating at D_{CJ} (steady detonation velocity that depends on the mixture stoichiometry and initial pressure, P_o , and temperature, T_o). The thermodynamic conditions immediately behind the leading shock correspond to the so-called von Neumann state (specified by subscript vN). The shock speed is then allowed to decay at a prescribed rate given by different mathematical forms: linear, exponential and power law (see next section for details). As the shock speed decreases, the conditions behind the shock change, and the gas in this region undergoes a volumetric expansion. Chemical reactions can no longer be considered to take place at constant volume or constant pressure, and the cooling of the gas needs to be taken into account. The form of the decay rate and imposed temperature drop could lead to quenching of the chemistry depending upon the initial conditions of the mixture. Figure 1 shows a schematic of the problem for illustrative purposes. It is assumed that the expansion is controlled only by the instantaneous conditions behind the shock. This imposes some simplification in particular the absence of a time lag due to perturbation propagation between the shock and the considered gas volume moving away. In the next subsection the methodology and calculation procedure are outlined in detail.

2.2. Methodology

Three mathematical forms of the shock wave velocity, U_s , decaying at different rates have been considered:

Linear:

$$U_s(t) = D_{CJ} - \alpha t \quad (1)$$

where $t = \tilde{t}/\tau_{Th}$ with \tilde{t} denoting the physical time. τ_{Th} is the time to thermicity peak considering an adiabatic constant pressure reactor model initially at the von Neumann state, and is used as our characteristic time scale. α is the velocity decay over one characteristic time, and has units of m/s.

Exponential:

$$U_S(t) = D_{CJ} \exp(-\beta t) \quad (2)$$

where β is the coefficient of exponential decay over one characteristic time, and is dimensionless.

Power law:

$$U_S(t^*) = D_{CJ} (t^*)^{-\delta} \quad (3)$$

δ is the power law exponent, and is dimensionless. The time scale for the power law is given by $t^* = (\tilde{t} + \tau_{Th}) / \tau_{Th}$.

The coefficients α , β , and δ are calculated separately for each initial condition, so that regardless of the mathematical form used for the decay rate, a given temperature drop, ΔT , is achieved through an isentropic expansion over a characteristic time, τ_{Th} . The non-dimensional time, by construction, is unity for the linear and exponential decay rates, and equals to 2 for the power law (i.e. $t=1$ and $t^*=2$).

The incident shock pressure which meets the specified temperature drop, $P_S(\Delta T)$, can be computed using the following isentropic relationship:

$$P_S(\Delta T) = P_{vN} \left(\frac{T_{vN} - \Delta T}{T_{vN}} \right)^{\frac{\gamma}{\gamma-1}} \quad (4)$$

The shock speed, $U_S(\Delta T)$, for which $P_S = P_S(\Delta T)$ is found using the 1-D normal shock equations and an iterative procedure.

The shock speed decay rate coefficients are obtained from [Equation 1](#) to [Equation 3](#) and are given by:

Linear:

$$\alpha(\Delta T) = \frac{D_{CJ} - U_S(\Delta T)}{t(\tau_{Th})} = D_{CJ} - U_S(\Delta T) \quad (5)$$

Exponential:

$$\beta(\Delta T) = \frac{\ln(D_{CJ}/U_S(\Delta T))}{t(\tau_{Th})} = \ln \left(\frac{D_{CJ}}{U_S(\Delta T)} \right) \quad (6)$$

Power law:

$$\delta(\Delta T) = \frac{\ln(U_S(\Delta T)/D_{CJ})}{-\ln(t^*(\tau_{Th}))} = \frac{\ln(D_{CJ}/U_S(\Delta T))}{\ln(2)} \quad (7)$$

Using the different decay rate formulations for the shock speed, the evolution of the post-shock pressure P_S is calculated using the 1-D normal shock equations. Based on this pressure history, the corresponding

specific volume evolution is computed assuming an isentropic expansion. The ignition delay-time is computed for an initial thermodynamic state at P_{vN} and T_{vN} and the specific volume variation along the isentrope previously computed from the shock wave decay rate. The final time of the computation, t_f , is calculated for each decay law as:

Linear:

$$t_{f, Lin} = \frac{D_{CJ} - U_S^{crit}}{\alpha(\Delta T)} \quad (8)$$

Exponential:

$$t_{f, Exp} = \frac{\ln(D_{CJ}/U_S^{crit})}{\beta(\Delta T)} \quad (9)$$

Power law:

$$t_{f, Pw}^* = \left(\frac{D_{CJ}}{U_S^{crit}} \right)^{1/\delta(\Delta T)} \quad (10)$$

where U_S^{crit} is the shock velocity at a Mach number $M_S=1.001$.

For the power law decay rate, non-physical values would be obtained in the range $t=[0+\epsilon, 1-\epsilon]$ with $\epsilon \ll 1$ (infinitely small increment) to avoid singularity at $t^*=0$. Consequently, the evolution of the shock wave speed was calculated for $t^* \geq 1$ and then, the physical time, \tilde{t} , was shifted back to zero by subtracting τ_{Th} : $\tilde{t} = t^* - 1$.

The ignition delay-time was defined in all cases as the time to thermicity peak, τ_{Th} . Quenching of the ignition process was detected when the difference between two consecutive points of the temperature profile was 0 K or negative. In this case, the delay-time is simply set to infinity.

2.3. Calculation procedure

A Matlab script has been implemented to perform the calculations which rely on several models from the Chemkin II library: Equil [7] for equilibrium state behind a CJ detonation; Shock [8] for flow state behind a normal shock; and Senkin [9] for homogeneous ignition under adiabatic conditions. The successive steps of the calculation procedure are listed below:

1. Calculate the Chapman-Jouguet velocity, D_{CJ} , using Equil.
2. Calculate the von Neumann state (P_{vN} and T_{vN}) for $U_S=D_{CJ}$ using Shock.
3. Calculate the adiabatic constant pressure ignition delay-time, τ_{Th} , at the von Neumann state using Senkin.
4. Calculate $P_S(\Delta T)$ using the isentropic relationship for a prescribed temperature drop, ΔT , using Equation 4.
5. Calculate the corresponding $U_S(\Delta T)$ using Shock and an iterative procedure.
6. Calculate the shock decay rates coefficients (α , β and δ) using Equation 5 to Equation 7.
7. Calculate t_f (or t_f^*) for all decay rates using Equation 8 to Equation 10.
8. Construct time vector in the range $[0, t_f]$.

9. Calculate shock velocity, U_S , corresponding to each element of the time vector using Equation 5 to Equation 7 based on the calculated shock speed decay rates (α , β and δ).
10. Calculate with Shock the incident shock pressure, $P_S(t)$, corresponding to each value of $U_S(t)$.
11. Calculate the evolution of the specific volume, v , considering the von Neumann state (P_{vN} and T_{vN}) as the starting point and the incident shock pressures, P_S . Isentropic law is considered to compute the evolution of the temperature.
12. Calculate the ignition delay-time in the expanding gas following the prescribed variation of the specific volume using Senkin with the Volume vs. time option (VTIM).

3. RESULTS AND DISCUSSION

3.1. Ignition delay-time under volumetric expansion

The ignition delay-time has been calculated for a stoichiometric hydrogen-air mixture initially at 300 K and at a pressure in the range 10-1013 kPa (with a 10 kPa increment). The detailed reaction model, and associated thermodynamics data, from Mével et al. [10, 11] has been employed for all the simulations. The initial thermodynamic state for the ignition calculations corresponded to the von Neumann state, i.e. pressure and temperature behind a shock propagating at the Chapman-Jouguet velocity. The normalized cooling rate was varied between 0 and 250 K/ τ_{Th} (with a 10 K/ τ_{Th} increment) for the linear and exponential decay. For the power law decay, the cooling rate was varied only in the range [120,250] K/ τ_{Th} (10 K/ τ_{Th} increment). This is because at low cooling rates, $t_{f,Pw}^*$ tends to infinity.

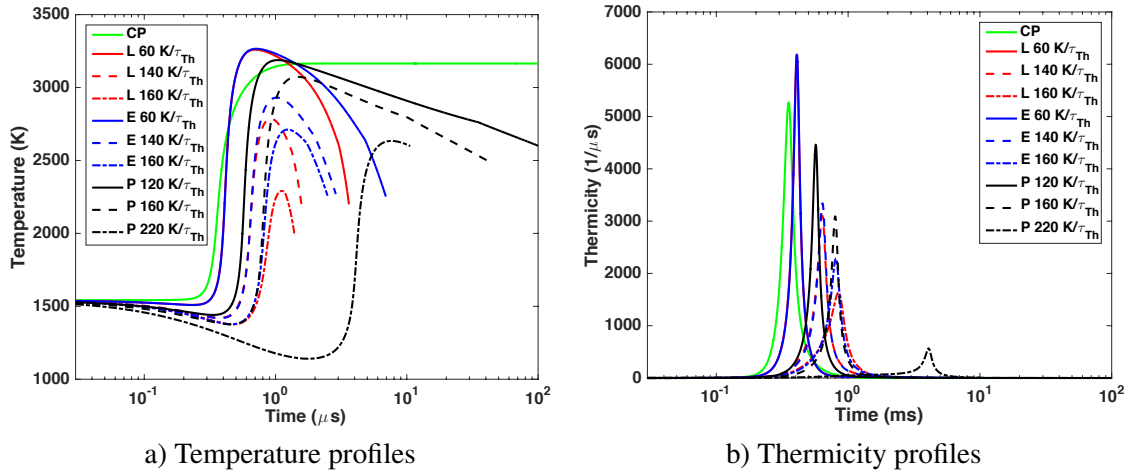


Figure 2: Temperature and thermicity profiles obtained for different cooling rates and mathematical forms of shock speed decay. Conditions: $\Phi=1$; $T_0=300$ K; $P_0=101$ kPa. E: exponential decay; L: linear decay; P: power law decay; CP: constant pressure.

Figure 2 shows the temperature and thermicity profiles obtained for different cooling rates and the three mathematical forms of shock speed decay. At low cooling rate, around 60 K/ τ_{Th} , the delay-time is only slightly influenced, $\sim 14\%$ longer, and the energy release rate in the VTIM simulation can exceed that in the CP simulation because the pressure increases during the heat release with the VTIM reactor model. At intermediate cooling rate, around 160 K/ τ_{Th} , the mathematical form of the shock speed decay does not influence significantly the time to ignition but the energy release rate is higher for the power law decay and exponential decay as compared to the linear decay (see black dashed lines and red and blue

dashed-dotted lines). At high cooling rate, $> 200 \text{ K}/\tau_{Th}$, the mixtures undergoing an expansion induced by the linear or exponential shock decay do not ignite, whereas the mixture undergoing an expansion induced by a power law decay still ignites but with a much lower energy release rate, 8-10 times lower at $220 \text{ K}/\tau_{Th}$ than for $120 \text{ K}/\tau_{Th}$.

The ignition delay-time results are summarized in Figure 3. Several features can be seen from the evolution of the ignition delay-time as a function of initial pressure under various cooling rate conditions: (i) the cooling induced by a power law shock decay is less efficient at quenching the ignition than the cooling induced by a linear or an exponential decay; (ii) the ignition process at low pressure, below 100 kPa, is the least sensitive to cooling; (iii) the ignition process at intermediate pressure, in the range 500-800 kPa, is the most sensitive to cooling.

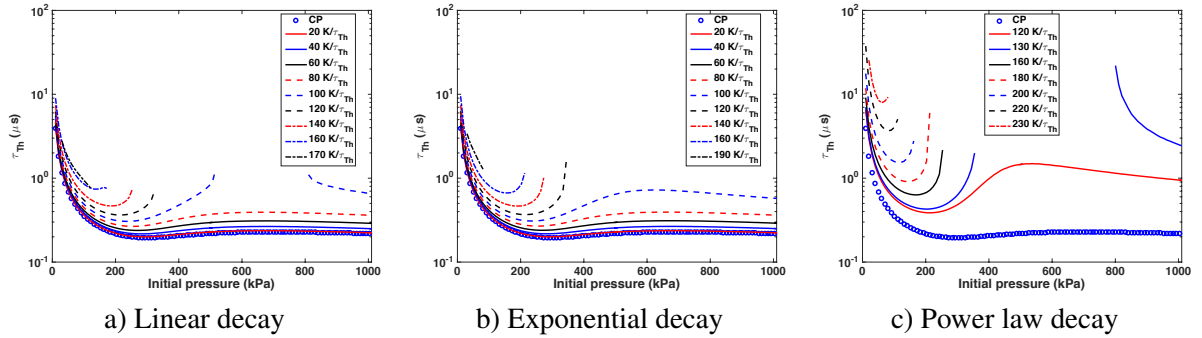


Figure 3: Evolution of the ignition delay-time at the von Neumann state as a function of initial pressure under volumetric expansion induced by shock speed decay. Initial conditions: $\Phi=1$; $T_0=300 \text{ K}$; $P_0=10\text{-}1013 \text{ kPa}$.

In order to explain these features, the adiabatic constant pressure ignition delay-time has been calculated with initial conditions following the isentropes described by the volumetric expansion processes that were considered to obtain Figure 3 a) to c). Figure 4 a) shows the evolution of the ignition delay-time along the three isentropes obtained by considering linear, exponential and power law shock speed decays. For a shock speed decay following a power law, the cooling rate is the fastest until τ_{Th} , our characteristic time scale, as compared to the linear and exponential decays. However, the cooling rate significantly drops after τ_{Th} for the power law decay, so that the delay-time curve demonstrates several changes of slope and τ_{Th} becomes orders of magnitude shorter than for the other decay laws for $t > 3$.

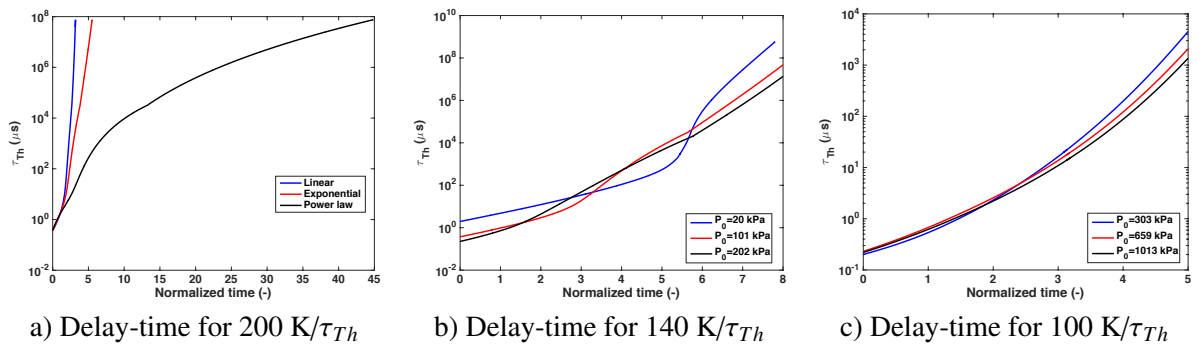


Figure 4: Effect a) of the mathematical form of shock speed decay rate, b) of the initial pressure in the low-pressure range, and c) of the initial pressure in the intermediate- and high-pressure ranges on the ignition delay-time along isentropes. Conditions before shock heating: $\Phi=1$; $T_0=300 \text{ K}$; a) $P_0=101 \text{ kPa}$, b) exponential decay rate for $P_0=20, 101, 202 \text{ kPa}$, and c) linear decay rate for $P_0=303, 659, 1013 \text{ kPa}$. The position along the isentrope is given as a function of the normalized time, t or t^* .

Figure 4 b) and c) show the evolution of the ignition delay-time along isentropes obtained by considering exponential or linear decays and different initial pressures. At low initial pressure, 20 kPa, the ignition process is taking place in the high-temperature regime. As the cooling is taking place, the ignition delay-time increases sharply around $t=5$ as the ignition process enters the low temperature regime (extended second explosion limit). At higher initial pressure, the ignition process enters this regime of lower reactivity earlier during the cooling phase, $t=3$ for $P_0=101$ kPa and $t=2$ for $P_0=202$ kPa. This slower increase of the delay-time during cooling leads to a higher reactivity at intermediate t for the low initial pressure case, which explains the weaker sensitivity to cooling. At intermediate and high initial pressure, the ignition delay-time varies monotonically along the three isentropes. At the von Neumann state and early stages of the cooling process, $t < 2$, the delay-time is the shortest for $P_0=303$ kPa and the longest for $P_0=659$ kPa. Because the delay-time increases continuously along the isentrope, the ignition process can survive only under low and moderate cooling rates. The highest sensitivity to cooling is observed for the conditions at which the delay-time is the longest at the beginning of the cooling phase.

3.2. Thermo-chemistry dynamics at near-critical conditions

In this section, the profiles for species, energy release rate, rate of species production and sensitivity coefficient are examined close to the critical conditions for quenching. All calculations were performed for an initial pressure of 101 kPa and a shock speed decay that follows a power law with cooling rates of 0, 200, 225 and 230 K/τ_{Th} .

As seen in Figure 5, which shows the species profiles for different cooling rates, the fast consumption of reactants and formation of active intermediate species is more and more delayed as the cooling rate is increased. At near critical conditions, cooling rate of 225 K/τ_{Th} , chemical activity demonstrates a runaway behavior just before the final time is reached. Beyond this cooling rate, no significant consumption of the reactants is observed within the time of the calculations.

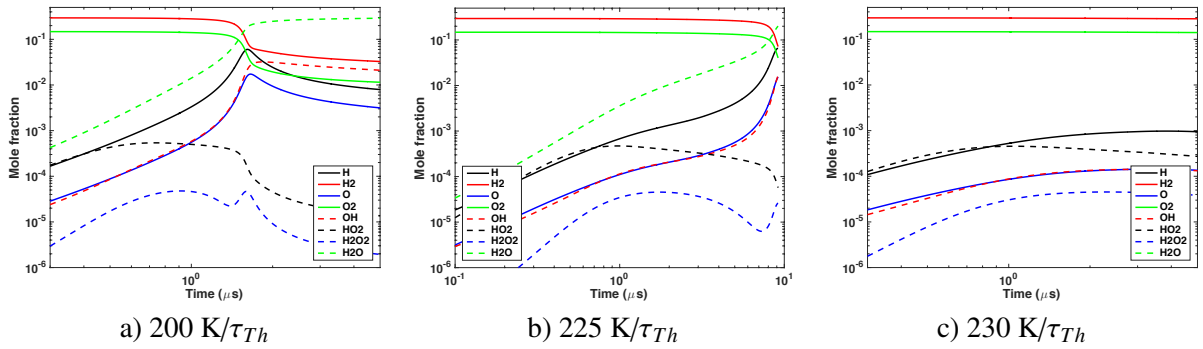


Figure 5: Species profiles obtained for different cooling rates around the critical conditions considering a power law shock speed decay. Conditions before shock heating: $\Phi=1$; $T_0=300$ K; $P_0=101$ kPa.

Figure 6 a) to c) show the profiles for the energy loss rate induced by the volumetric expansion and for the chemical energy release obtained for several cooling rates around the critical conditions. In Figure 6 d) to f), the individual contributions of the most important reactions to the chemical energy production and consumption are given. In Figure 6 g) to i), the rate of production per reaction for the hydroxyl radicals are shown. The energy loss rate due to expansion was calculated using

$$q_{Cool} = \frac{C_p \Delta T}{M_{v,sp} \Delta t}, \quad (11)$$

where C_p is the molar heat capacity at constant pressure (J/K mol), $\Delta T/\Delta t$ is the temperature temporal gradient (K/s), M is the molar mass (kg/mol), and v_{sp} is the specific volume (cm³/kg).

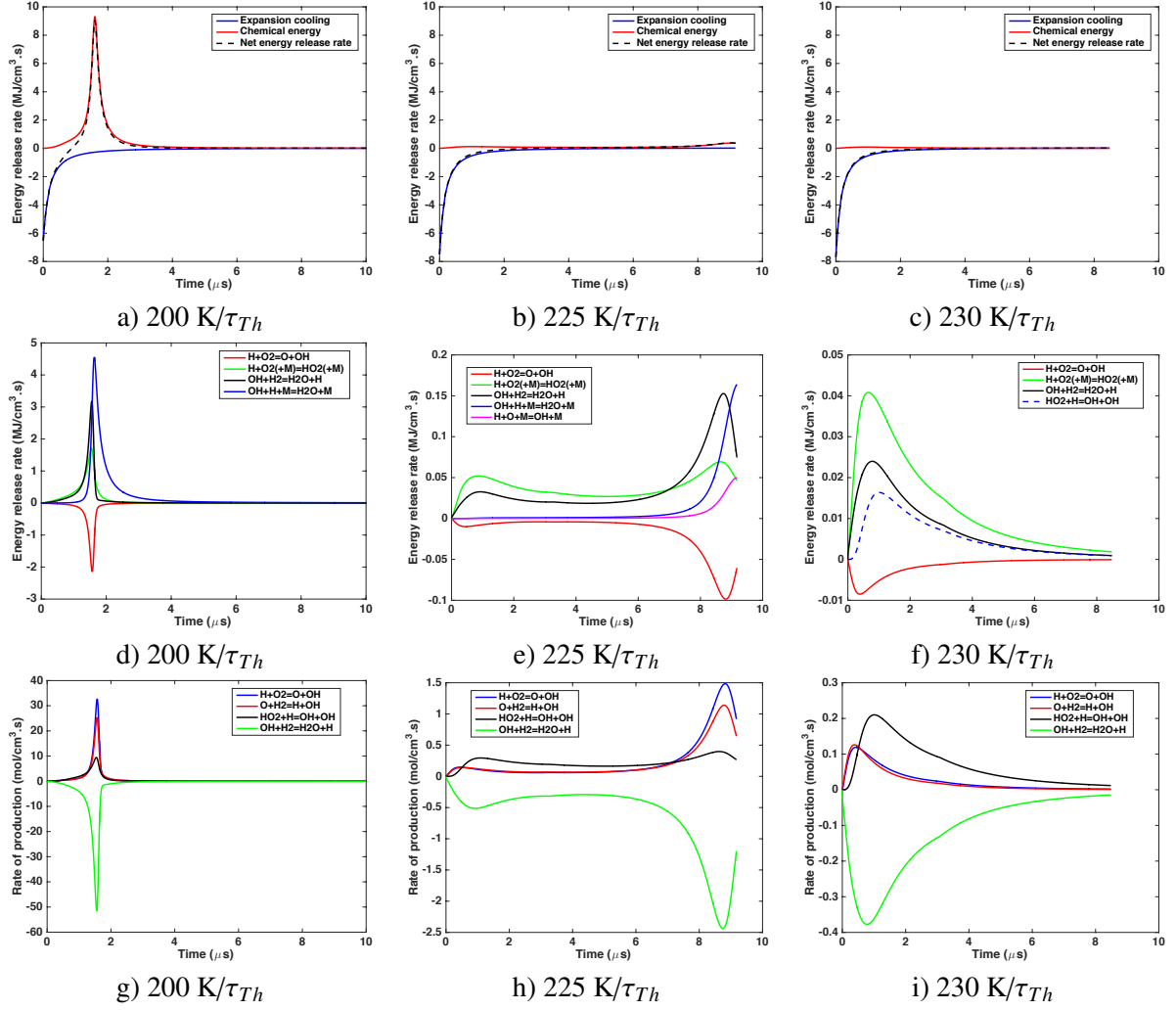


Figure 6: Profiles of energy and OH radical rate of production and consumption obtained for different cooling rates around the critical conditions considering a power law shock decay. a) to c): total cooling and chemical energy release rates. d) to f): chemical energy release rate per reaction. g) to i): OH rate of production. Conditions before shock heating: $\Phi=1$; $T_0=300$ K; $P_0=101$ kPa.

For a cooling rate below the critical condition, the chemical energy release rate rapidly exceeds the cooling rate which leads to ignition. Because of the power law shape of the energy loss profile, the cooling rate strongly decreases after about 1-1.5 μ s. The chemical energy release is mainly driven by $H+O_2(+M)=HO_2(+M)$ during the induction period, and by $OH+H_2=H_2O+H$ and $OH+H+M=H_2O+M$ during the ignition stage. The production of OH radicals is through the classical chain branching mechanism, $H+O_2=O+OH$ and $O+H_2=H+OH$, and the contribution of the sequence $H+O_2(+M)=HO_2(+M)$ followed by $HO_2+H=OH+OH$ is limited. At the critical cooling rate, the overall chemical reaction rate is much reduced, more than one order of magnitude, as seen from the energy release rate per reaction profiles. During the induction period, which extends over approximately 7 μ s, the primary source of chemical energy release is $H+O_2(+M)=HO_2(+M)$, and the production of OH radical is dominated by a linear chain process: $HO_2+H=OH+OH$. Around this time, the cooling rate has decreased enough so that the slow energy release can overcome losses and accelerate the reaction rate and energy release and induce ignition. As ignition is taking place, just before the end of the calculation, the primary reaction

for energy production becomes $\text{OH} + \text{H} + \text{M} = \text{H}_2\text{O} + \text{M}$ and the energy consumption and OH production by the chain branching reaction $\text{H} + \text{O}_2 = \text{O} + \text{OH}$ increase sharply. For a cooling rate above the critical value, the chemical energy release rate never exceeds the energy loss rate which maintains the global reaction rate at a low level, two orders of magnitude lower for the energy release rate per reaction. The primary reaction for energy production is $\text{H} + \text{O}_2(+\text{M}) = \text{HO}_2(+\text{M})$ with a peak of energy release at about $1 \mu\text{s}$. The peak of OH radical production rate also occurs at $1 \mu\text{s}$ and is mainly due to $\text{HO}_2 + \text{H} = \text{OH} + \text{OH}$. Following this instant, the energy release rate continuously drops which indicates overall chemistry suppression or quenching. The results of the sensitivity analyses on OH radical are shown in Figure 7. It is seen that, as the cooling rate is increased and approaches the critical conditions, the sensitivity coefficient for $\text{H} + \text{O}_2 = \text{O} + \text{OH}$ and $\text{H} + \text{O}_2(+\text{M}) = \text{HO}_2(+\text{M})$ strongly increases and decreases, respectively. This results indicate an increased importance of the competition between the chain branching and linear chain processes for the production of OH radicals as the critical conditions are approached.

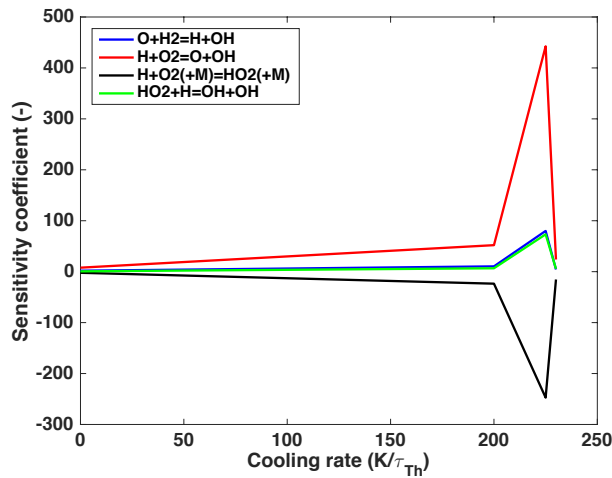


Figure 7: Evolution of the maximum absolute sensitivity coefficient on OH radicals for four important reactions as a function of cooling rate considering a power law shock speed decay. Conditions before shock heating: $\Phi=1$; $T_0=300 \text{ K}$; $P_0=101 \text{ kPa}$.

4. CONCLUSION

The ignition of hydrogen-air mixtures under volumetric expansion induced by shock speed decay has been studied. Three mathematical forms for the shock speed decay have been employed: linear, exponential and power law. It was shown that for a given cooling rate, normalized by the time to ignition under constant pressure conditions, the expansion induced by a power law decay was the least efficient at quenching ignition. It was also shown that the most sensitive conditions to cooling were for intermediate initial pressures, $P_0=500\text{--}800 \text{ kPa}$, and that the least sensitive conditions were for low initial pressures, $P_0 < 100 \text{ kPa}$. This complex response of the ignition process of hydrogen-air mixtures to volumetric expansion is explained by the highly non-monotonous evolution of the ignition delay-time with pressure and temperature.

REFERENCES

1. C. A. Eckett, J. J. Quirk, J. E. Shepherd, The role of unsteadiness in direct initiation of gaseous detonations, *Journal of Fluid Mechanics* 421 (2000) 147–183.
2. M. Arienti, J. Shepherd, A numerical study of detonation diffraction, *Journal of Fluid Mechanics* 529 (2005) 117–146.

3. B. Maxwell, M. Radulescu, Ignition limits of rapidly expanding diffusion layers: Application to unsteady hydrogen jets, *Combustion and Flame* 158 (10) (2011) 1946–1959.
4. E. Lundstrom, A. Oppenheim, On the influence of non-steadiness on the thickness of the detonation wave, in: *Proceedings of the Royal Society of London A: Mathematical, Physical and Engineering Sciences*, Vol. 310, The Royal Society, 1969, pp. 463–478.
5. M. I. Radulescu, B. M. Maxwell, Critical ignition in rapidly expanding self-similar flows, *Physics of Fluids* 22 (6) (2010) 066101.
6. L. He, P. Clavin, On the direct initiation of gaseous detonations by an energy source, *Journal of fluid mechanics* 277 (1994) 227–248.
7. A. Lutz, F. Rupley, R. Kee, Equil: A chemkin implementation of stanjan for computing chemical equilibria, Tech. rep., Sandia National Laboratories (1992).
8. R. Mitchell, R. Kee, Shock: a general purpose computer code for predicting chemical kinetic behavior behind incident and reflected shocks, Tech. Rep. 82-8205, Sandia National Laboratories (1982).
9. A. Lutz, R. Kee, J. Miller, Senkin : a fortran program for predicting homogeneous gas phase chemical kinetics with sensitivity analysis, Tech. Rep. Sand87-8248, Sandia International Laboratories (1992).
10. R. Mével, S. Javoy, F. Lafosse, N. Chaumeix, G. Dupré, C. E. Paillard, Hydrogen-nitrous oxide delay time: shock tube experimental study and kinetic modelling, *Proceedings of The Combustion Institute* 32 (2009) 359–366.
11. R. Mével, S. Javoy, G. Dupré, A chemical kinetic study of the oxidation of silane by nitrous oxide, nitric oxide and oxygen, *Proceedings of The Combustion Institute* 33 (2011) 485–492.